Supporting Information

Size effect of nickel from nanoparticles to clusters to single atoms for electrochemical CO_2 reduction

Qin Pan,[a] Yang Chen,[a,b]* Hui Li,[c] Guanghuan Ma,[a] Shuoshuo Jiang,[a] Xin Cui,[a] Lei Zhang,[c] Yuxin Bao,[a] Tianyi Ma[c,]*

[a] Institute of Clean Energy Chemistry, Key Laboratory for Green Synthesis and Preparative Chemistry of Advanced Materials of Liaoning Province, College of Chemistry, Liaoning University, Shenyang, 110036, China

[b] CAS Key Laboratory of Science and Technology on Applied Catalysis, Dalian Institute of Chemical Physics, Chinese Academy of Sciences, Dalian, 116023, China

[c] School of Science, RMIT University, Melbourne, VIC 3000, Australia

1. Experimental section

1.1 Materials

$Ni(NO_3)_2 \cdot 6H_2O$ (98%, Tianjin beilian reagents), $Zn(NO_3)_2 \cdot 6H_2O$ (99%, AHX), 2-methylimidazole (98%, Macklin), Nickel(II) acetate tetrahydrate (99%, Aladdin), 1,4,7,10-tetraazacyclododecane (>97%, Aladdin), methanol (99.5%, Macklin), hexane (≥99.0%, Fuyu chemical reagents), carbon paper (MAYA-CR-9247), Nafion solution (5 wt.%, D520), ethanol (≥99.4%, Shanghai chemical reagents) were used without purification.

1.2 Electrochemical measurements

Linear scanning voltammograms (LSV) tests were performed in 0.5 M $KHCO_3$ solution with a scan rate of 10 mV/s. The electrochemical surface area (ECSA) is proportional to the value of the double-layer capacitance (C_{dl}), which can be obtained from cyclic voltammetry (CV) curves at diverse scan rates. Electrochemical impedance spectroscopy (EIS) measurements were conducted at an open-circuit voltage (OCP) with an amplitude of 5 mV over the frequency of 0.1~100000 Hz.

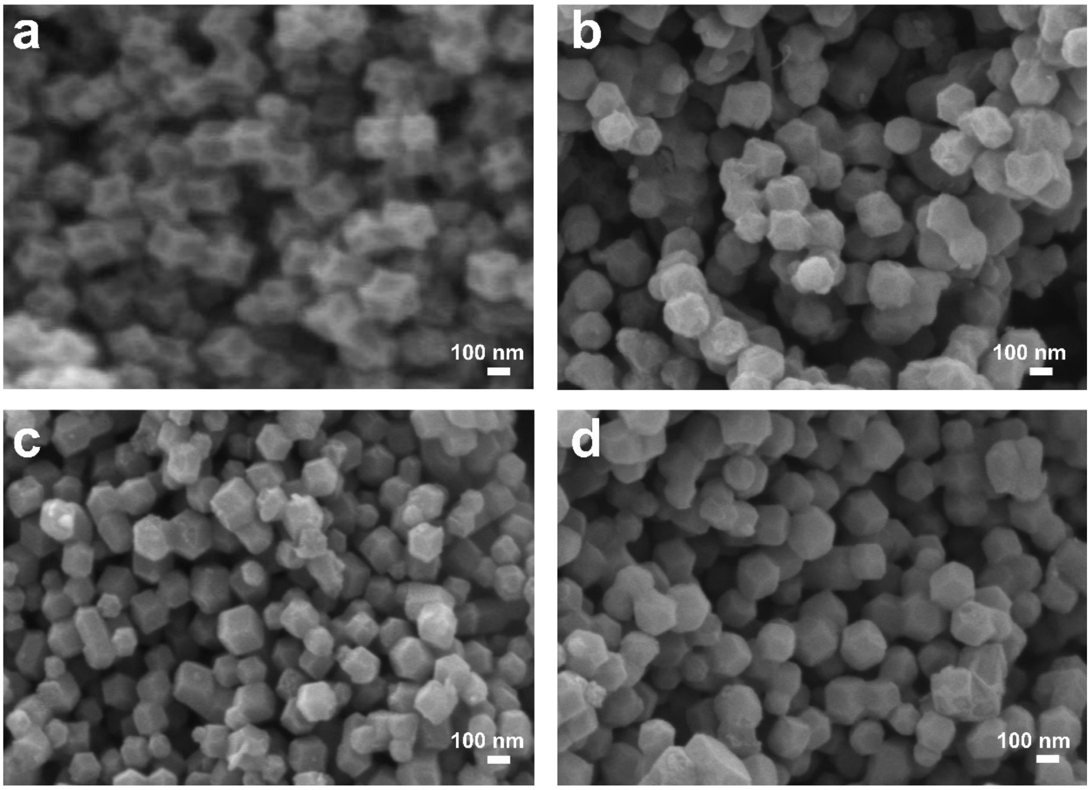

Fig. S1. SEM images of (a) Ni SAC, (b) Ni cluster, (c) Ni NP, and (d) N-C.

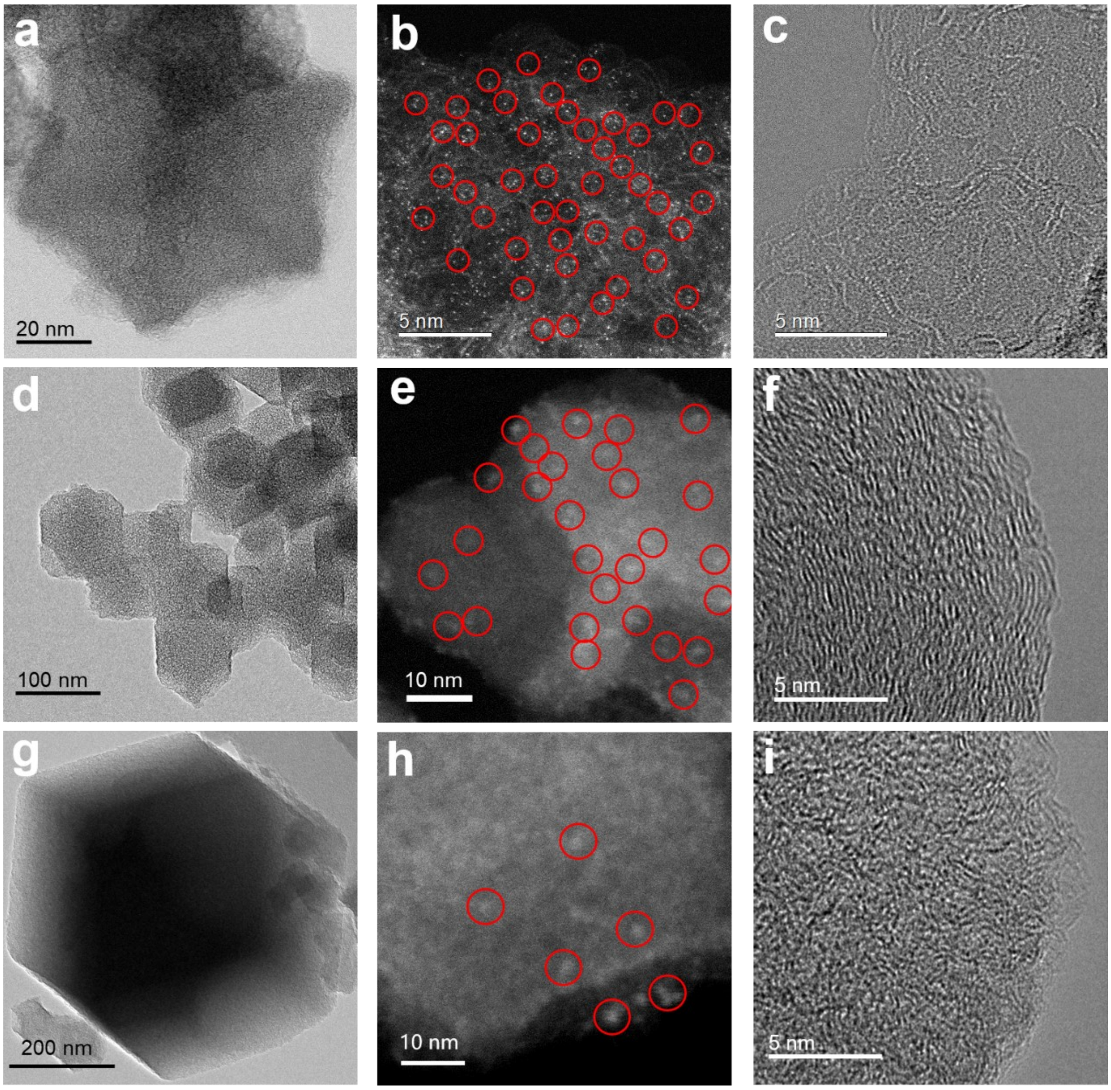

Fig. S2. (a-c) TEM and AC-HAADF-STEM images of Ni SAC, (d-f) TEM and HAADF-STEM images of Ni cluster, (g-i) TEM and HAADF-STEM images of Ni NP.

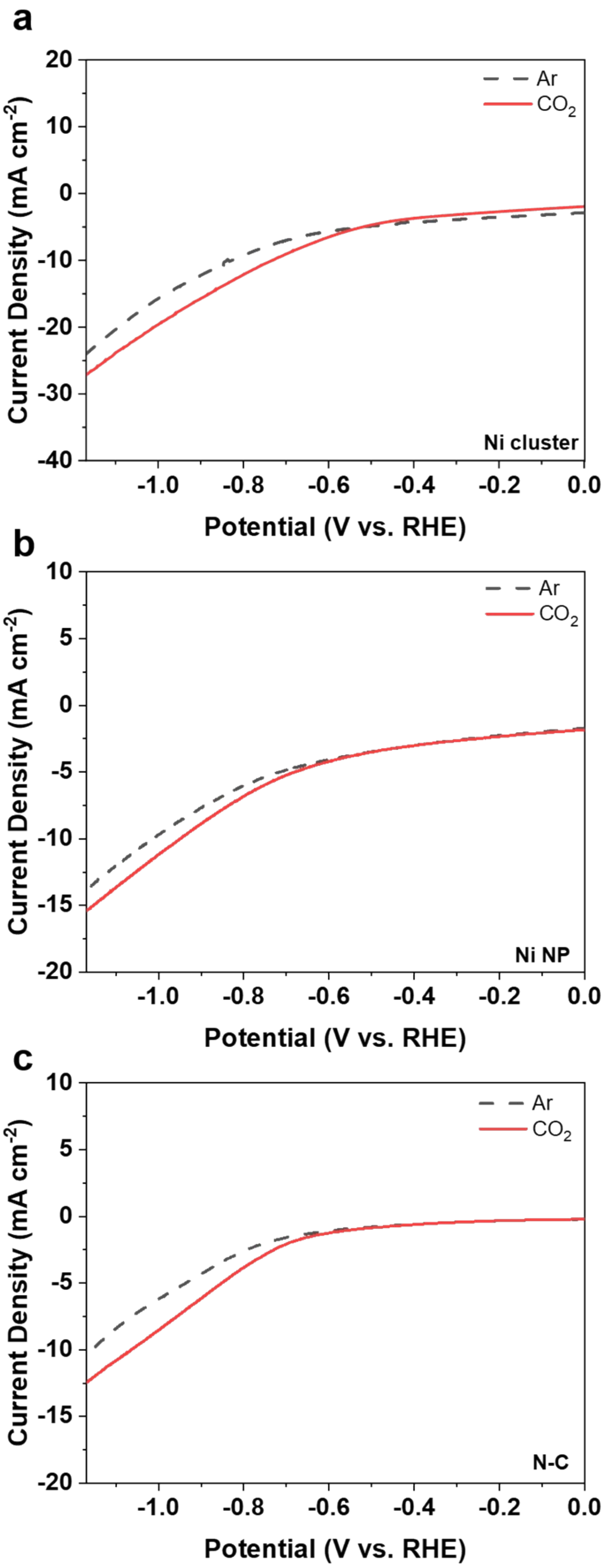

Fig. S3. LSV curves of different catalysts in the Ar-saturated (dotted line) and CO_2-saturated (solid line) 0.5 M $KHCO_3$ electrolyte at a scan rate of 10 mV s^{-1} of (a) Ni cluster, (b) Ni NP, and (c) N-C.

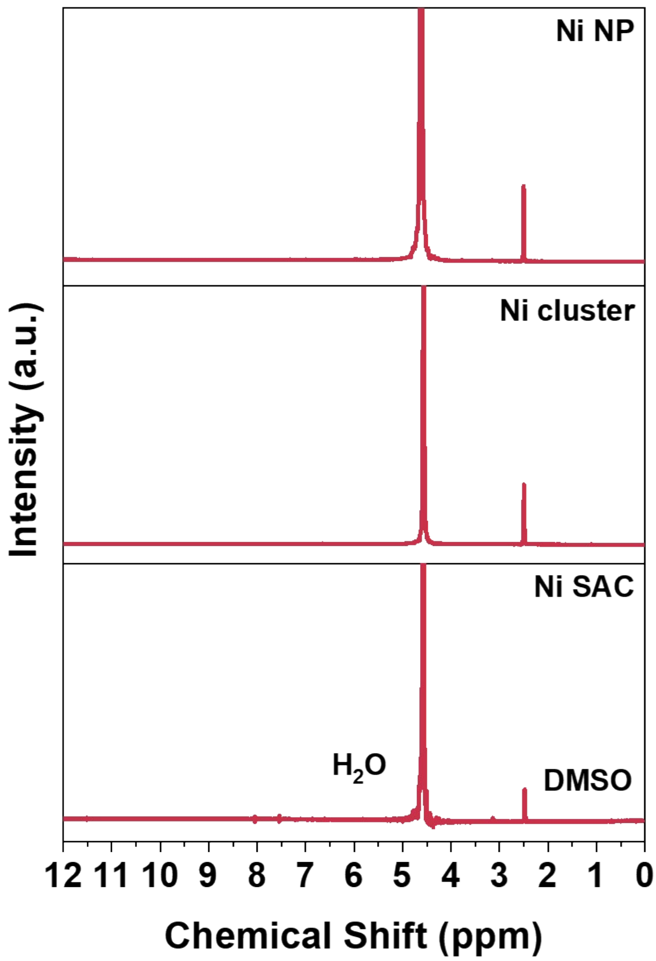

Fig. S4. ^{1}H NMR spectrum of the electrolyte after CO_2RR over Ni SAC, Ni cluster, and Ni NP for 1 h at an applied potential of -0.8 V vs. RHE.

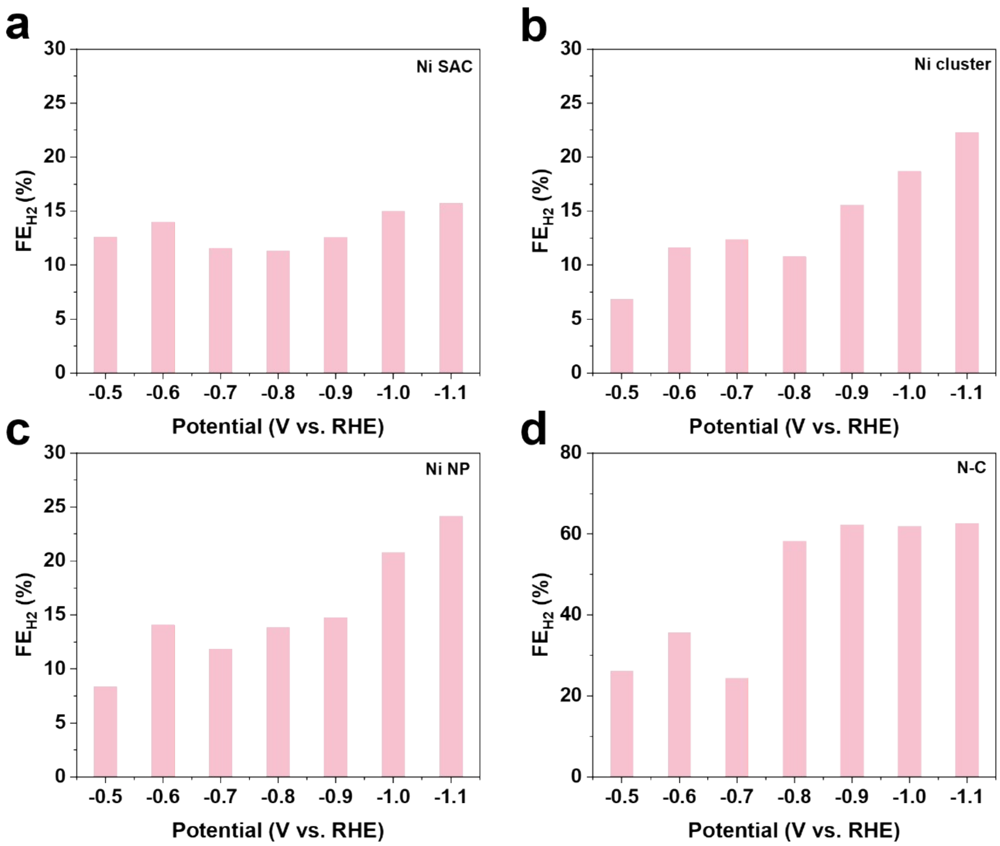

Fig. S5. FE_{H2} in CO_2-saturated 0.5 M $KHCO_3$ at different applied potentials of (a) Ni SAC, (b) Ni cluster, (c) Ni NP, and (d) N-C, respectively.

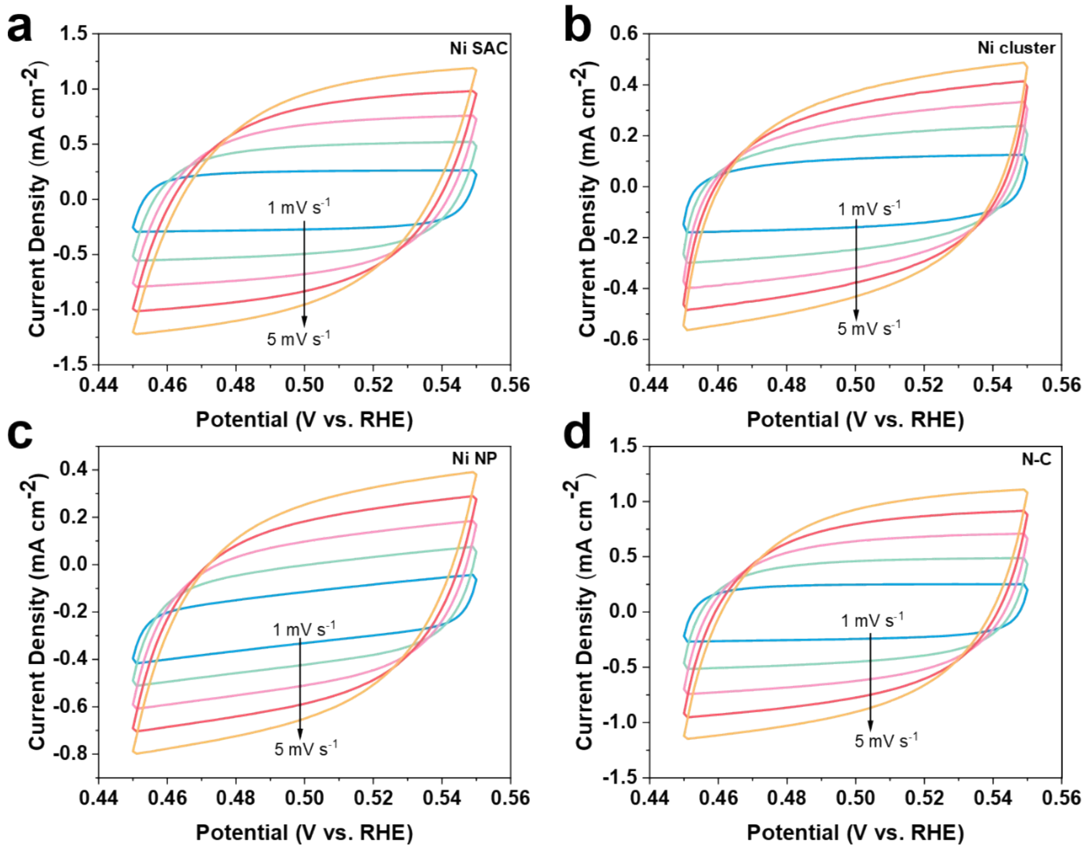

Fig. S6. CV measurements with scan ranging from 1 to 5 mV s^{-1} with an interval of 1 mV s^{-1} at the potential range of 0.45 V to 0.55 V vs. RHE for (a) Ni SAC, (b) Ni cluster, (c) Ni NP, and (d) N-C, respectively.

Table S1. Physiochemical properties of the prepared Ni SAC, Ni cluster, Ni NP, and N-C catalysts.

Catalysts	Ni loading (wt.%)	BET surface area（m^2/g）	Pore volume (cm^3/g)	Pore size (nm)
Ni SAC	1.68	901	0.57	2.53
Ni cluster	1.66	1406	0.94	2.67
Ni NP	1.85	898	0.56	2.49
N-C	-	841	0.49	2.32

Table S2. Comparison of the electrochemical performance of metal-N-C catalysts for CO_2RR.

Catalyst	Size (nm)	Metal loading (wt.%)	E (V vs. RHE)	FE_{CO} (%)	J_{CO} (mA cm^{-2})	TOF (h^{-1})	Ref.
Ni SAC	-	1.68	-0.8	85	12	3554.5	This work
Ni cluster	1.1	1.66	-0.8	68	8.2	1773.7	This work
Ni NP	15.3	1.85	-0.8	59	4.0	1249.5	This work
NiPc/CNT	-	0.17	-0.79	97	8	4000	1
Ni-NC@Ni	0.2	1	-0.78	87.4	24	~1752	2
Ni-SNC	-	2.2	-0.8	95	11	~109.5	3
Ni@N-C	7	3.9	-0.8	90	17	~795.4	4
Fe-N-C	-	1.5	-0.6	91	7.5	~520.9	5
Fe/NG	-	1.25	-0.6	80	1.75	~72.9	6
Fe-CNPs	40	0.24	-0.58	98.8	5.4	~234.4	7
Fe-N-G	-	0.36	-0.58	94	2.3	1630	8
FeNPs-NC	20	-	-0.6	93	2.5	-	9
Fe_2C-Cs	1.07	1.37	-0.7	97.1	8	-	10
Co-N_3	-	8.01	-0.66	42	7	69.4	11
CoPc	-	0.46	-0.8	90	28	~3346	12
Zn NPs	6.8	0.2	-1.1	70	2.8	-	13

References

1 Y. J. Sa, H. Jung, D. Shin, H. Y. Jeong, S. Ringe, H. Kim, Y. J. Hwang and S. H. Joo, *ACS Catal.*, 2020, **10**, 10920-10931.

2 Y. He, Y. Li, J. Zhang, S. Wang, D. Huang, G. Yang, X. Yi, H. Lin, X. Han, W. Hu, Y. Deng and J. Ye, *Nano Energy*, 2020, **77**, 105010.

3 X. Yang, J. Cheng, H. Lv, X. Yang, L. Ding, Y. Xu, K. Zhang, W. Sun and J. Zhou, *Chem. Eng. J.*, 2022, **450**, 137950.

4 F. Wang, G. Wang, P. Deng, Y. Chen, J. Li, D. Wu, Z. Wang, C. Wang, Y. Hua and X. Tian, *Small*, 2023, **19**, 2301128.

5 T. N. Huan, N. Ranjbar, G. Rousse, M. Sougrati, A. Zitolo, V. Mougel, F. Jaouen and M. Fontecave, *ACS Catal.*, 2017, **7**, 1520-1525.

6 C. Zhang, S. Yang, J. Wu, M. Liu, S. Yazdi, M. Ren, J. Sha, J. Zhong, K. Nie, A. S. Jalilov, Z. Li, H. Li, B. I. Yakobson, Q. Wu, E. Ringe, H. Xu, P. M. Ajayan and J. M. Tour, *Adv. Energy Mater.*, 2018, **8**, 1703487.

7 C. Hu, S. Bai, L. Gao, S. Liang, J. Yang, S.-D. Cheng, S.-B. Mi and J. Qiu, *ACS Catal.*, 2019, **9**, 11579-11588.

8 F. Pan, B. Li, E. Sarnello, Y. Fei, X. Feng, Y. Gang, X. Xiang, L. Fang, T. Li, Y. H. Hu, G. Wang and Y. Li, *ACS Catal.*, 2020, **10**, 10803-10811.

9 Q. Fan, G. Bao, X. Chen, Y. Meng, S. Zhang and X. Ma, *ACS Catal.*, 2022, **12**, 7517-7523.

10 J. Su, D. Pan, Y. Dong, Y. Zhang, Y. Tang, J. Sun, L. Zhang, Z. Tian and L. Chen, *Adv. Energy Mater.*, 2023, **13**, 2204391.

11 Y. Pan, R. Lin, Y. J. Chen, S. J. Liu, W. Zhu, X. Cao, W. X. Chen, K. L. Wu, W. C. Cheong, Y. Wang, L. R. Zheng, J. Luo, Y. Lin, Y. Q. Liu, C. G. Liu, J. Li, Q. Lu, X. Chen, D. S. Wang, Q. Peng, C. Chen and Y. D. Li, *J. Am. Chem. Soc.*, 2018, **140**, 4218-4221.

12 M. Huang, B. Chen, H. Zhang, Y. Jin, Q. Zhi, T. Yang, K. Wang and J. Jiang, *Small Methods*, 2024, 2301652.

13 H. S. Jeon, I. Sinev, F. Scholten, N. J. Divins, I. Zegkinoglou, L. Pielsticker and B. R. Cuenya, *J. Am. Chem. Soc.*, 2018, **140**, 9383-9386.